

Rational Design of Fluorescein-Based Fluorescence Probes. Mechanism-Based Design of a Maximum Fluorescence Probe for Singlet Oxygen

Kumi Tanaka, Tetsuo Miura, Naoki Umezawa, Yasuteru Urano, Kazuya Kikuchi,
Tsunehiko Higuchi, and Tetsuo Nagano*

Contribution from the Graduate School of Pharmaceutical Sciences, The University of Tokyo,
7-3-1 Hongo, Bunkyo-ku, Tokyo 113-0033, Japan

Received October 2, 2000. Revised Manuscript Received January 6, 2001

Abstract: Fluorescein is one of the best available fluorophores for biological applications, but the factors that control its fluorescence properties are not fully established. Thus, we initiated a study aimed at providing a strategy for rational design of functional fluorescence probes bearing fluorescein structure. We have synthesized various kinds of fluorescein derivatives and examined the relationship between their fluorescence properties and the highest occupied molecular orbital (HOMO) levels of their benzoic acid moieties obtained by semiempirical PM3 calculations. It was concluded that the fluorescence properties of fluorescein derivatives are controlled by a photoinduced electron transfer (PET) process from the benzoic acid moiety to the xanthen ring and that the threshold of fluorescence OFF/ON switching lies around -8.9 eV for the HOMO level of the benzoic acid moiety. This information provides the basis for a practical strategy for rational design of functional fluorescence probes to detect certain biomolecules. We used this approach to design and synthesize 9-[2-(3-carboxy-9,10-dimethyl)anthryl]-6-hydroxy-3H-xanthen-3-one (DMAX) as a singlet oxygen probe and confirmed that it is the most sensitive probe currently known for $^1\text{O}_2$. This novel fluorescence probe has a 9,10-dimethylanthracene moiety as an extremely fast chemical trap of $^1\text{O}_2$. As was expected from PM3 calculations, DMAX scarcely fluoresces, while DMAX endoperoxide (DMAX-EP) is strongly fluorescent. Further, DMAX reacts with $^1\text{O}_2$ more rapidly, and its sensitivity is 53-fold higher than that of 9-[2-(3-carboxy-9,10-diphenyl)anthryl]-6-hydroxy-3H-xanthen-3-ones (DPAXs), which are a series of fluorescence probes for singlet oxygen that we recently developed. DMAX should be useful as a fluorescence probe for detecting $^1\text{O}_2$ in a variety of biological systems.

Introduction

Fluorescence probes are excellent sensors for biomolecules, being sensitive, fast-responding, and capable of affording high spatial resolution via microscopic imaging.¹ Among many fluorescent compounds, fluorescein is known to have a high quantum yield of fluorescence (ϕ) in aqueous solution and to be excitable at long wavelength,² and it is the most widely used fluorophore for labeling and sensing biomolecules.³ Long-wavelength light does not cause severe cell damage and is free from interference by autofluorescence of biological molecules.⁴ Further, excitation around 490 nm is convenient for fluorescence confocal microscopy using an Ar⁺ ion laser.

Nevertheless, only limited empirical information is available about the factors that control the fluorescence properties of fluorescein. Munkholm et al. reported that the nitrogen electron

density of aminofluorescein and its derivatives is the most important factor determining the quantum efficiency of fluorescence (ϕ); that is, aminofluorescein has a low ϕ value of 0.015, whereas its amide derivatives fluoresce strongly.⁵ However, to our knowledge, little more is known about the relationship between the chemical structures of fluorescein derivatives and their fluorescent properties. Thus, we initiated a study aimed at providing a strategy for rational design of functional fluorescence probes based on the fluorescein structure. Further, using the developed strategy, we designed and synthesized the most sensitive fluorescence probe for $^1\text{O}_2$ so far known.

Results and Discussion

Photoinduced Electron Transfer⁶ as a Mechanism That Controls the Fluorescence Properties of Fluorescein Derivatives. Recently we reported a series of fluorescence probes for $^1\text{O}_2$, 9-[2-(3-carboxy-9,10-diphenyl)anthryl]-6-hydroxy-3H-xanthen-3-ones (DPAXs).⁷ DPAXs were the first chemical traps for $^1\text{O}_2$ that permit fluorescence detection. They react with $^1\text{O}_2$ to produce DPAX endoperoxides (DPAX-EPs). Although DPAXs are fluorescein derivatives, DPAXs themselves scarcely fluoresce, while DPAX-EPs are strongly fluorescent. However, the mechanisms accounting for the diminution of fluorescence in DPAXs and its enhancement in DPAX-EPs remain unclear. Our working hypothesis is that the fluorescence properties of fluorescein derivatives are controlled by the photoinduced

(1) Bissell, R. A.; de Silva, A. P.; Gunaratne, H. Q. N.; Lynch, P. L. M.; McCoy, C. P.; Maguire, G. E. M.; Sandanayake, K. R. A. S. In *Fluorescent Chemosensors for Ion and Molecule Recognition*; Czarnik, A. W., Ed.; ACS Symposium Series 538; American Chemical Society: Washington, DC, 1993; Chapter 9.

(2) Sun, W.; Gee, K. R.; Klaubert, D. H.; Haugland, R. P. *J. Org. Chem.* **1997**, *62*, 6469–6475.

(3) (a) Kojima, H.; Nakatsubo, N.; Kikuchi, K.; Kawahara, S.; Kirino, Y.; Nagoshi, H.; Hirata, Y.; Nagano, T. *Anal. Chem.* **1998**, *70*, 2446–2453. (b) Kojima, H.; Urano, Y.; Kikuchi, K.; Higuchi, T.; Nagano, T. *Angew. Chem., Int. Ed.* **1999**, *38*, 2899–2901. (c) Mizukami, S.; Kikuchi, K.; Higuchi, T.; Urano, Y.; Mashima, T.; Tsuruo, T.; Nagano, T. *FEBS Lett.* **1999**, *453*, 356–360.

(4) Tsien, R. Y.; Waggoner, A. In *Handbook of Biological Confocal Microscopy*; Pawley, J. B., Ed.; Plenum Press: New York, 1995; pp 267–279.

(5) Munkholm, C.; Parkins, D. R.; Walt, D. R. *J. Am. Chem. Soc.* **1990**, *112*, 2608–2612.

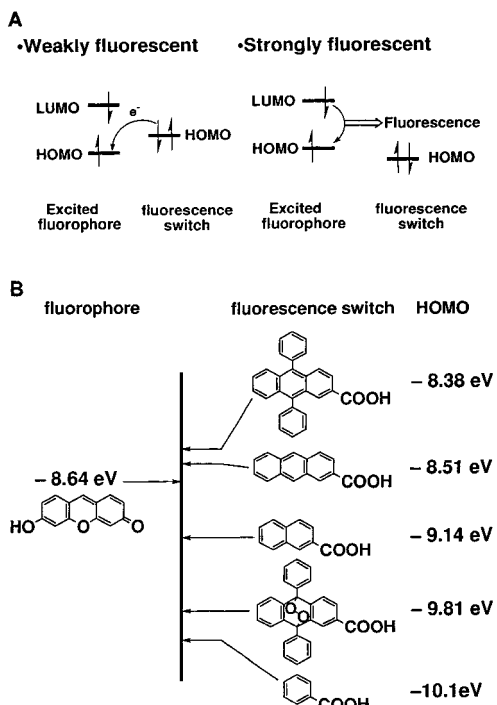


Figure 1. Frontier orbital energy diagram. (A) Illustration of the thermodynamic situation of the fluorescence OFF/ON switch including the PET process. (B) HOMO levels of 6-hydroxy-3H-xanthen-3-one (fluorophore) and benzoic acid moieties (fluorescence switch) in various fluorescein derivatives. These values were obtained from semiempirical PM3 calculations.

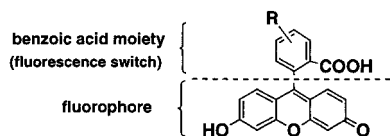
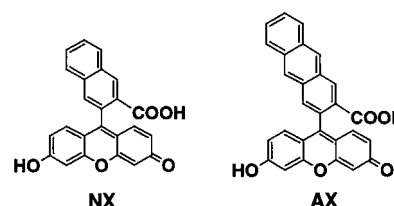


Figure 2. Fluorescein structure divided into two parts, the fluorescence switch and the fluorophore.

electron transfer (PET) process from the benzoic acid moiety to the fluorophore, the xanthen ring (Figure 1A). PET is a widely accepted mechanism for fluorescence quenching, in which electron transfer from the PET donor to the excited fluorophore diminishes the fluorescence of the fluorophore. We consider that it is appropriate to divide the fluorescein structure into two parts, i.e., the benzoic acid moiety as the PET donor and the xanthen ring as the fluorophore (Figure 2), because only small alterations in absorbance were observed among fluorescein and its derivatives and the dihedral angle between the benzoic acid moiety and the xanthen ring is almost 90° , as found by X-ray analysis,⁸ which suggests that there is little ground-state interaction between these two parts. Our hypothesis is that if the highest occupied molecular orbital (HOMO) energy

level of the benzoic acid moiety is high enough for electron transfer to the excited xanthen ring, the ϕ value will be small. In other words, fluorescein derivatives with high ϕ values must have benzoic moieties with low HOMO energy levels. The HOMO energy levels of 3-aminobenzoic acid, 3-benzamido-benzoic acid, 9,10-diphenylanthracene-2-carboxylic acid (DPA-COOH), and 9,10-diphenylanthracene-9,10-endoperoxide-2-carboxylic acid (DPA-EP-COOH), which are the benzoic moieties of aminofluorescein, benzamidofluorescein, DPAX, and DPAX-EP, respectively, were estimated by semiempirical (PM3) calculations. DPA-COOH and aminobenzoic acid, which are the benzoic acid moieties of weakly fluorescent fluorescein derivatives, have relatively higher HOMO levels than DPA-EP-COOH and amidobenzoic acid (Table 1). These results were in accordance with our hypothesis. Further, to confirm this hypothesis, we synthesized 9-[2-(3-carboxy)naphthyl]-6-hydroxy-3H-xanthen-3-one (NX) and 9-[2-(3-carboxy)anthryl]-6-hydroxy-3H-xanthen-3-one (AX). It is well known that expand-



ing the size of aromatic conjugates makes their HOMO levels higher, as does introducing electron-donating substituents. So we anticipated that naphthoic acid and anthracene-2-carboxylic acid would have higher HOMO levels than benzoic acid and that the fluorescence properties of NX and AX would differ from those of fluorescein.

Their absorbance and fluorescence properties as well as the HOMO levels of their benzoic acid moieties are summarized in Table 1. The excitation maximum (Ex_{max}) and emission maximum (Em_{max}) were not much altered among these fluorescein derivatives. However, the ϕ values were greatly altered: NX is highly fluorescent, whereas AX is almost nonfluorescent. Thus, a small change in the size of conjugated aromatics, namely from naphthalene to anthracene, causes a great alteration of fluorescence properties. When HOMO levels of benzoic acid moieties were compared, we found that HOMO levels of benzoic acid and naphthoic acid, which are present in highly fluorescent fluorescein and NX, are lower than that of the xanthen ring, while the HOMO level of anthracenecarboxylic acid, which is present in the scarcely fluorescent AX, is higher than that of the xanthen ring (Figure 1B). These results are consistent with the idea that a PET process controls the fluorescence properties of fluorescein derivatives and that these properties can be predicted from the HOMO level of the benzoic acid moiety, with a threshold around -8.9 eV. This, in turn, provides a basis for developing novel fluorescence probes with fluorescein-derived structure.

Design of DMAX and Its Fluorescence Properties. Singlet oxygen ($^1\text{O}_2$) is one of the active species for oxidation in biological systems, together with superoxide ion, hydroxyl radical, hydrogen peroxide, etc. Many researchers have investigated the reactivity of $^1\text{O}_2$ toward organic substrates,⁹ as well as its possible role in biological systems.¹⁰ However, some results are still controversial, mainly because of the lack of a reliable detection method. $^1\text{O}_2$ has high reactivity and a short

(6) (a) de Silva, A. P.; Gunarathe, H. Q. N.; Gunnlaugsson, T.; Huxley, A. J. M.; McCoy, C. P.; Rademacher, J. T.; Rice, T. E. *Chem. Rev.* **1997**, *97*, 1515–1566. (b) Bissell, R. A.; de Silva, A. P.; Gunarathe, H. Q. N.; Lynch, P. L. M.; McCoy, C. P.; Maguire, G. E. M.; Sandanayake, K. R. A. S. In *Fluorescent Chemosensors for Ion and Molecule Recognition*; Czarnik, A. W., Ed.; ACS Symposium Series 538; American Chemical Society: Washington DC, 1993; Chapter 4. (c) Bissell, R. A.; de Silva, A. P.; Gunarathe, H. Q. N.; Lynch, P. L. M.; Maguire, G. E. M.; Sandanayake, K. R. A. S. *Chem. Soc. Rev.* **1992**, *21*, 187–195. (d) Hirano, T.; Kikuchi, K.; Urano, Y.; Higuchi, T.; Nagano, T. *Angew. Chem., Int. Ed.* **2000**, *39*, 1052–1054.

(7) Umezawa, N.; Tanaka, K.; Urano, Y.; Kikuchi, K.; Higuchi, T.; Nagano, T. *Angew. Chem., Int. Ed.* **1999**, *38*, 2899–2901.

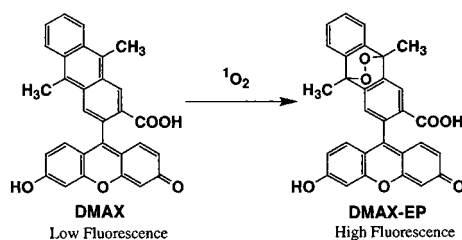
(8) Yamaguchi, K.; Tamura, Z.; Maeda, M. *Acta Crystallogr.* **1997**, *C53*, 284.

(9) (a) Frimer, A. A., Ed. *Singlet Oxygen*; CRC Press: Boca Raton, FL, 1997. (b) Prein, M.; Adam, W. *Angew. Chem., Int. Ed.* **1996**, *35*, 477–484.

Table 1. Absorbance and Fluorescence Properties of Fluorescein Derivatives, DMAX and DMAX-EP

	absorbance maximum (nm)	molar absorption coefficient ($\times 10^4 \text{ M}^{-1} \text{ cm}^{-1}$)	emission maximum (nm)	quantum efficiency	calculated HOMO level of its benzoic acid moiety (eV)
fluorescein ^{a,d}	492	8.0	517	0.85	-10.1
4-benzamidofluorescein ^b	490	nd ^e	nd	0.79	-9.29
DPAX-1-EP ^{c,d}	494	7.9	515	0.53	-9.81
NX ^d	492	6.9	512	0.83	-9.14
DMAX-EP ^d	492	7.1	515	0.81	-9.83
4-aminofluorescein ^b	490	nd	nd	0.015	-8.90
DPAX-1 ^{c,d}	493	6.1	516	0.007	-8.38
AX ^d	492	6.5	510	0.003	-8.51
DMAX ^d	492	6.0	517	0.015	-8.26

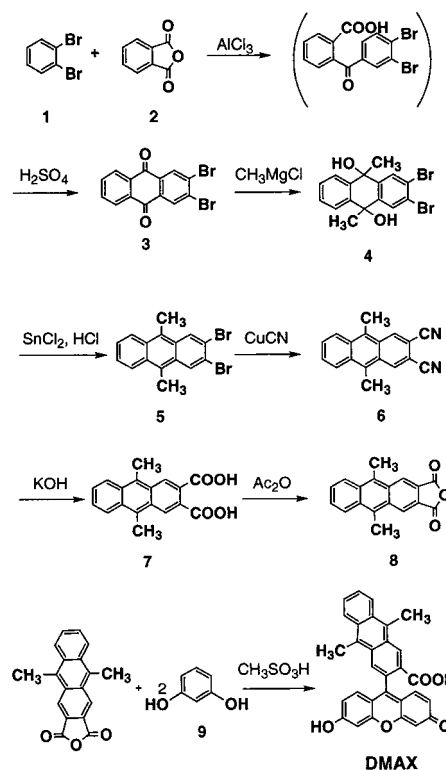
^a References 2 and 4. ^b Reference 5. Data were measured in 0.1 M phosphate buffer, pH 7.5. ^c Reference 7. ^d Data were measured in 0.1 M NaOH. ^e nd, not determined.

Scheme 1. Reaction of DMAX with Singlet Oxygen

lifetime ($2 \mu\text{s}$ in water),¹¹ and the only tools currently available for the real-time bioimaging assay of $^1\text{O}_2$ production in living cells are DPAXs. Although DPAXs are useful for detection of $^1\text{O}_2$, they have some limitations in application to biological systems, especially with regard to their sensitivity.

We utilized our above-mentioned hypothesis to design a novel fluorescence probe with much higher sensitivity for $^1\text{O}_2$, with a faster rate of formation of endoperoxide upon reaction with $^1\text{O}_2$, namely 9-[2-(3-carboxy-9,10-dimethyl)anthryl]-6-hydroxy-3H-xanthen-3-one (DMAX). We predicted that DMAX should react rapidly with $^1\text{O}_2$ and that DMAX endoperoxide (DMAX-EP) should be strongly fluorescent, because dimethylantracene-2-carboxylic acid (DMA-COOH) and DMA-COOH endoperoxide (DMA-EP-COOH) were indicated to be suitable for OFF/ON fluorescence switching by semiempirical PM3 calculation (Table 1, Scheme 1). DMA is known to react very rapidly ($k = 9.1 \times 10^8 \text{ M}^{-1} \text{ s}^{-1}$ in water) with $^1\text{O}_2$ specifically to give the corresponding 9,10-endoperoxide, DMA-EP.¹¹ This reaction rate is much faster than that of DPA (for example, $1.0 \times 10^6 \text{ M}^{-1} \text{ s}^{-1}$ in benzene; no data available in water),¹² so we expected DMAX would show much greater sensitivity than DPAXs for $^1\text{O}_2$. With regard to the reaction rate, the classic singlet oxygen trap 1,3-diphenylisobenzofuran (DPBF) has a comparable rate constant ($9.6 \times 10^8 \text{ M}^{-1} \text{ s}^{-1}$ in water), but DPBF reacts with other reactive oxygen species, i.e., hydroxyl radical and hypochlorite, to yield the same product. Since we required a specific probe for singlet oxygen, we chose DMA as the singlet oxygen trap. Furthermore, the hydrophobicity of DMAX is less than that of DPAXs, which is important for use in biological samples.

DMAX was prepared according to usual methods with an excess of resorcinol and 9,10-dimethylantracene-2,3-dicarboxylic anhydride,^{2,13} as shown in Scheme 2. DMAX-EP was

Scheme 2. Synthetic Scheme of DMAX

prepared from DMAX with the $\text{Mo}^{6+}-\text{H}_2\text{O}_2$ system.¹⁴ Values of $E_{x_{\text{max}}}$, $E_{m_{\text{max}}}$, ϕ , and ϵ are summarized in Table 1. $E_{x_{\text{max}}}$, ϵ , and $E_{m_{\text{max}}}$ were similar for DMAX and DMAX-EP, but, as was expected from the PM3 calculations, DMAX itself is almost nonfluorescent and DMAX-EP is highly fluorescent. The quantum yield of DMAX-EP is almost 1.5 times higher than that of DPAX-1-EP, which means that the sensitivity of DMAX is greater than that of DPAX-1, apart from any consideration of reaction rates.

$^1\text{O}_2$ Detection in Aqueous Media. Next we tried to detect $^1\text{O}_2$ in aqueous media under neutral conditions (pH 7.4). 3-(1,4-Dihydro-1,4-epidioxo-4-methyl-1-naphthyl)propionic acid (EP-1) was used as a $^1\text{O}_2$ source.^{14,15} EP-1 is a water-soluble compound, producing $^1\text{O}_2$ and 3-(4-methyl-1-naphthyl)propionic acid (N-1) thermally. Various concentrations of EP-1 were added to a buffer solution of DMAX or DPAX-1 ($10 \mu\text{M}$, 0.1%

(10) (a) Brivida, K.; Klotz, L. O.; Sies, H. *J. Biol. Chem.* **1997**, *378*, 1259–1265. (b) Scharffetter-Kochanek, K.; Wlaschek, M.; Brivida, K.; Sies, H. *FEBS Lett.* **1993**, *331*, 304–306. (c) Grether-Beck, S.; Olaizola-Horn, S.; Schmitt, H.; Grewe, M.; Jahnke, A.; Johnson, J. P.; Brivida, K.; Sies, H.; Krutmann, J. *Proc. Natl. Acad. Sci. U.S.A.* **1996**, *93*, 14586–14591.

(11) Usui, Y.; Tsukada, M.; Nakamura, H. *Bull. Chem. Soc. Jpn.* **1978**, *51*, 379–384.

(12) Wilkinson, F.; Brummer, J. G. *J. Phys. Ref. Data* **1981**, *10*, 809–999.

(13) Confalone, P. N. *J. Heterocycl. Chem.* **1997**, *27*, 31.

(14) Aubry, J. M.; Cazin, B.; Duprat, F. *J. Org. Chem.* **1989**, *54*, 726–728.

(15) (a) Saito, I.; Matsuura, T.; Inoue, K. *J. Am. Chem. Soc.* **1983**, *105*, 3200–3206. (b) Saito, I.; Matsuura, T.; Inoue, K. *J. Am. Chem. Soc.* **1981**, *103*, 188–190.

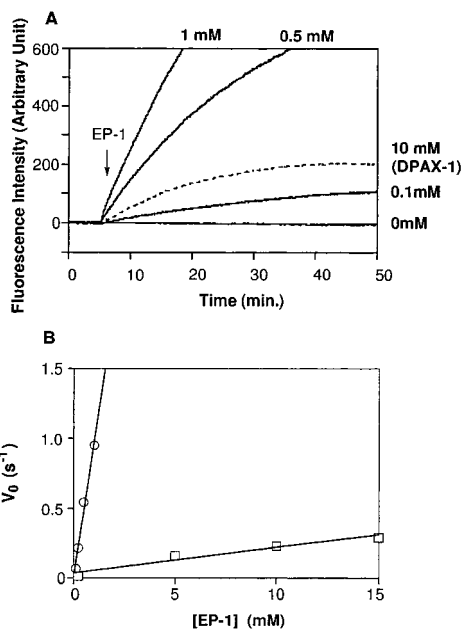


Figure 3. Reaction of DMAX and DPAX-1 with singlet oxygen. (A) Time course of the fluorescence intensity (Ex = 491 nm, Em = 520 nm) in the reaction of DMAX (full line) and DPAX-1 (broken line) with ¹O₂ generated from EP-1. Various concentrations of EP-1 were added at the point indicated by the arrow. (B) V_0 indicates the initial rates of the fluorescence increase of DMAX and DPAX-1. The reaction was performed at 37 °C in 0.1 M sodium phosphate buffer at pH 7.4.

DMSO), and the reactions were performed at 37 °C in 0.1 M sodium phosphate buffer at pH 7.4. Fluorescence intensity (Ex = 491 nm, Em = 520 nm) was monitored as a function of time. As shown in Figure 3 A, fluorescence intensity was increased depending on the concentration of EP-1, and DMAX was clearly more sensitive than DPAX-1. The fluorescence increase paralleled DMAX-EP and DPAX-1-EP formation, as confirmed by HPLC (Figure 4). To measure the rate constants of DMAX-EP and DPAX-1-EP formation and to elucidate whether DMAX can detect ¹O₂ quantitatively or not, we examined the correlation between the concentration of EP-1 and the initial rate of fluorescence augmentation. Figure 3B shows a good linear relationship between these two parameters, which suggests that ¹O₂ can be detected quantitatively with DMAX. The slopes were 1.0 and 1.9×10^{-2} (arbitrary unit) s⁻¹ [EP-1 (mM)]⁻¹ for DMAX and DPAX-1, respectively. These results indicate that DMAX is 53-fold more sensitive than DPAX-1. From the fluorescence intensity–concentration relationships of DMAX-EP and DPAX-1-EP, the ¹O₂ lifetime, and the ¹O₂ formation rate from EP-1, we determined that the reaction rate constants of DMAX and DPAX-1 with ¹O₂ were 2.5×10^7 and 8.1×10^5 M⁻¹ s⁻¹, respectively. The reaction rate constants of DMAX and DPAX-1 are somewhat smaller than those of DMA and DPA. This might be due to the effect of the electron-withdrawing carboxylic acid attached to the anthracene ring. However, DMAX has a 31-fold faster rate constant and is 53-fold more sensitive than DPAX-1. To our knowledge, there are no chemical traps for ¹O₂ which have a faster rate constant and better selectivity for ¹O₂ than DMA. In addition, the fluorescence intensity of DMAX did not change upon reaction with 1.0 mM H₂O₂, 0.1 mM nitric oxide, and 0.2 mM superoxide, confirming the specificity of DMAX for ¹O₂. We consider that DMAX is the best fluorescence reagent for ¹O₂ detection currently available.

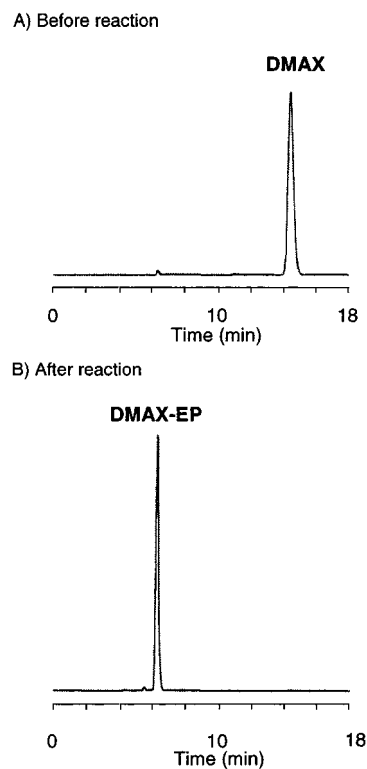


Figure 4. HPLC chromatogram of DMAX with singlet oxygen. DMAX was exposed to ¹O₂ generated from the H₂O₂/MoO₄²⁻ system. (A) Before the addition of H₂O₂, (B) After the addition of H₂O₂. Column: Inertsil ODS-3 (4.6 × 250 mm). Eluent: CH₃CN/100 mM sodium phosphate buffer (pH 7.4) = 2/5; flow rate = 1.0 mL/min; detection wavelength = 492 nm (absorption).

Conclusion

We synthesized various kinds of fluorescein derivatives, including NX and AX, and examined the relationship between their fluorescence properties and the HOMO levels of their benzoic acid moieties obtained by semiempirical PM3 calculations. The results are consistent with our hypothesis that the fluorescence properties of fluorescein derivatives are determined by a PET process from the benzoic acid moiety. This provides a practical strategy for rational design of functional fluorescence probes to detect certain biomolecules; that is, the threshold level for the HOMO level of the benzoic acid moiety calculated with the PM3 method is around -8.9 eV. The validity of our strategy was confirmed by using it to develop a novel fluorescence probe, DMAX, for ¹O₂. DMAX reacts with ¹O₂ more rapidly, and its sensitivity is 53-fold higher than that of DPAXs. These results indicate that DMAX is an excellent fluorescence probe for ¹O₂, and we suggest that it should be widely useful in biological systems. Our strategy should be applicable to develop fluorescein-derived functional indicators for a wide range of applications.

Experimental Section

Materials. *o*-Xylene, 2,3-naphthalenecarboxylic anhydride, and methanesulfonic acid were purchased from Tokyo Chemical Industries Co., Ltd. 1,2-Dibromobenzene and phthalic anhydride were purchased from Wako Pure Chemical Industries Ltd. Methylmagnesium chloride was purchased from Aldrich Chemical Co. Inc. Except for *o*-xylene, all of them were used without further purification. Benzene, *o*-xylene, methanol, THF, and DMF were used after distillation. Other materials were of the best grade available and were used without further purification.

Instruments. NMR spectra were recorded on a JEOL JNM-LA300 instrument at 300 MHz for ¹H NMR, and at 75 MHz for ¹³C NMR. Mass spectra (MS) were measured with a JEOL JMS-DX300 for EI

and a JEOL SX-102A for FAB. UV-visible spectra were obtained on a Shimadzu UV-1600. Fluorescence spectroscopic studies were performed on a Hitachi F4500. Determinations of reaction rate constants were performed on a Perkin-Elmer LS-50B.

Preparation of 2-(3',4'-Dimethylbenzoyl)benzoic Acid. Aluminum(III) chloride (15 g) was added to a suspension of phthalic anhydride (7.5 g, 50.6 mmol) in *o*-xylene (60 mL). The mixture was refluxed for 10 min, and 50 g of ice was added. The resulting mixture was treated with concentrated HCl, taken up in ether, and extracted with 2 M NaOH. The aqueous solution was washed with ether and acidified to pH ~2.5 with cold 6 M HCl. The resulting mixture was extracted with ether. The organic layer was washed with brine, dried over MgSO₄, filtered, and evaporated to afford a light yellow powder (4.78 g, yield 37%). ¹H NMR (DMSO-*d*₆): δ 2.23 (s, 3H), 7.22–7.30 (m, 2H), 7.35 (d, 1H, *J* = 7.3 Hz), 7.46 (s, 1H), 7.72–7.30 (m, 2H), 7.96 (d, 1H, *J* = 7.3 Hz). MS (EI⁺): *m/z* 254 (M⁺).

Preparation of 2,3-Dimethylantraquinone.¹⁶ 2-(3',4'-Dimethylbenzoyl)benzoic acid (4.7 g, 18.5 mmol) dissolved in 25.5 mL of concentrated sulfuric acid was warmed gradually to 125 °C over 1 h, kept at this temperature for 30 min, and then poured onto ice. The precipitated light gray powder was collected by filtration, washed with water, dried, and purified by silica gel chromatography (CH₂Cl₂/*n*-hexane, 1:1), to afford a light yellow powder containing a small amount of 1,2-dimethylantraquinone. Isomerically pure 2,3-dimethylantraquinone was obtained by recrystallization. A solution containing boiling acetic acid (12 mL per gram of the isomeric mixture) was filtered, and then the filtrate was allowed to cool and kept cool for 1 h. The resultant crystals were collected, washed with acetic acid, and dried in air oven to afford yellow needles (2.0 g, yield 46%). ¹H NMR (CDCl₃): δ 2.25 (s, 6H), 7.76–7.79 (m, 2H), 8.06 (s, 2H), 8.28–8.31 (m, 2H). MS (EI⁺): *m/z* 236 (M⁺). Mp: 185 °C.

Preparation of Anthraquinone-2,3-dicarboxylic Acid. 2,3-Dimethylantraquinone (3.3 g, 14.0 mmol) was added to a stirred solution of 8.10 g of Na₂Cr₂O₇ in 43 mL of water buffered with 5.33 g of NaH₂PO₄·2H₂O. The suspension thus obtained was quickly introduced into a stainless steel autoclave. The vessel was then heated to 250 °C for 20 h under stirring. After cooling to room temperature, the reaction mixture was treated with excess sodium sulfite and extracted with 2 M NaOH, and the aqueous layer was acidified to pH ~2 with cold 6 M HCl. The precipitate was collected by filtration, dried, purified by silica gel chromatography (CH₂Cl₂/methanol, 9:1), and recrystallized from acetic acid to afford light yellow crystals (392 mg, yield 9.5%). ¹H NMR (DMSO-*d*₆): δ 7.97–8.00 (m, 2H), 8.31–8.34 (m, 2H), 8.58 (s, 2H). MS (EI⁺): *m/z* 278 (M⁺ – H₂O).

Preparation of 2,3-Anthracenedicarboxylic Acid. Anthraquinone-2,3-dicarboxylic acid (392 mg, 1.31 mmol) was mixed with a large excess of zinc dust (2.5 g), dissolved in 14% ammonia solution (40 mL), and refluxed for 2 h. 2,3-Anthracenedicarboxylic acid was precipitated from the hot filtered solution by the addition of hydrochloric acid (335 mg, yield 95%). ¹H NMR (DMSO-*d*₆): δ 7.58–7.61 (m, 2H), 8.13–8.16 (m, 2H), 8.47 (s, 2H), 8.77 (s, 2H). MS (FAB⁺): *m/z* 267 (M⁺ + 1).

Preparation of 2,3-Anthracenedicarboxylic Anhydride. A suspension of 2,3-anthracenedicarboxylic acid (32 mg, 0.12 mmol) in acetyl chloride (1.2 mL) was refluxed for 1 h. The resulting clear solution was cooled to 4 °C to afford 2,3-anthracenedicarboxylic anhydride as a yellow precipitate (21 mg, yield 70%). ¹H NMR (CDCl₃): δ 7.72–7.75 (m, 2H), 8.23–8.26 (m, 2H), 8.77 (s, 2H), 8.80 (s, 2H). MS (FAB⁺): *m/z* 249 (M⁺ + 1). Mp: >300 °C.

Preparation of 2,3-Dibromoanthraquinone (3). Aluminum(III) chloride (4.4 g, 33.0 mmol) was added to a suspension of phthalic anhydride **2** (2.24 g, 15.1 mmol) in 2,3-dibromobenzene **1** (6 mL). The resulting mixture was heated at 150 °C for 1 h and then treated with 2 M HCl and extracted with benzene. The benzene layer was extracted with 2 M NaOH. The aqueous layer was acidified to pH ~2.5 with cold 6 M HCl. The resulting mixture was extracted with ether. The organic layer was washed with brine, dried over MgSO₄, filtered, and evaporated to afford a crude product. This was dissolved in

concentrated sulfuric acid (20 mL). The solution was warmed gradually to 125 °C over 1 h, kept at this temperature for 30 min, and then poured onto ice. The precipitated light gray powder was collected by filtration, washed with water, dried, and purified by silica gel chromatography (CH₂Cl₂/*n*-hexane, 2:1) to afford a light yellow powder (1.38 g, yield 25%). ¹H NMR (CDCl₃): δ 7.83–7.86 (m, 2H), 8.30–8.33 (m, 2H), 8.53 (s, 2H). MS (EI⁺): *m/z* 364:366:368 = 1:2:1 (M⁺). Mp: >300 °C.

Synthesis of 2,3-Dibromo-9,10-dihydroxy-9,10-dimethyl-9,10-dihydroanthracene (4). Methylmagnesium chloride (3 M in THF, 4.5 mL) was gradually added to a solution of **3** (1.22 g, 3.33 mmol) in dry THF (150 mL). The mixture was refluxed for 4 h under an Ar atmosphere. Aqueous ammonium chloride was added, and the whole was evaporated to a small volume. The resulting mixture was extracted with CH₂Cl₂. The organic layer was washed with brine, dried over Na₂SO₄, filtered and evaporated. The crude compound was purified by silica gel chromatography (CH₂Cl₂) to afford a light yellow powder (995 mg, yield 75%). ¹H NMR (CDCl₃): *cis*, δ 1.63 (s, 6H), 7.41–7.45 (m, 2H), 7.79–7.83 (m, 2H), 8.11 (s, 2H); *trans*, δ 1.86 (s, 6H), 7.41–7.45 (m, 2H), 7.79–7.83 (m, 2H), 8.01 (s, 2H). MS (EI⁺): *m/z* 396:398:400 = 1:2:1 (M⁺). Mp: 125 °C.

Synthesis of 2,3-Dibromo-9,10-dimethylantracene (5).¹⁷ A mixture of **4** (1.08 g, 2.71 mmol) in 28 mL of acetic acid, 12.8 g of stannous(II) chloride dihydrate, and 12 mL of concentrated hydrochloric acid was refluxed for 1 h under an Ar atmosphere. The cooled solution was poured into 500 mL of water, and the solid product was collected. The resulting solid was purified by silica gel chromatography (CH₂Cl₂/hexane, 1:2) to afford a yellow powder (744 mg, yield 78%). ¹H NMR (CDCl₃): δ 3.04 (s, 6H), 7.54–7.57 (m, 2H), 8.28–8.31 (m, 2H), 8.62 (s, 2H). MS (EI⁺): *m/z* 362:364:366 = 1:2:1 (M⁺). Mp: 151 °C.

Synthesis of 9,10-Dimethylantracene-2,3-dicarbonitrile (6). A stirred mixture of **5** (730 mg, 2.00 mmol) and cuprous(I) cyanide (694 mg, 7.74 mmol) in dimethylformamide (45 mL) was refluxed for 9 h under an Ar atmosphere. The reaction mixture was cooled to room temperature, and 14% aqueous ammonium solution (50 mL) was added to it. The precipitate was collected, washed with water, and dried. The crude product was purified by silica gel chromatography (CH₂Cl₂/hexane, 2:5) to afford a yellow powder (255 mg, yield 50%). ¹H NMR (CDCl₃): δ 3.14 (s, 6H), 7.71–7.76 (m, 2H), 8.39–8.43 (m, 2H), 8.86 (s, 2H). MS (EI⁺): 256 (M⁺). Mp: 266 °C dec.

Synthesis of 9,10-Dimethyl-2,3-anthracenedicarboxylic Acid (7). A solution of **6** (330 mg, 1.29 mmol) in 50 mL of *n*-butanolic potassium hydroxide (3 M) was refluxed for 10 h under an Ar atmosphere. The solution was acidified with concentrated HCl and extracted with ether. The organic layer was washed with brine, dried over Na₂SO₄, filtered, and evaporated. The resulting solid was purified by silica gel chromatography (CH₂Cl₂/MeOH, 20:1) to afford a yellow powder (268 mg, yield 71%). ¹H NMR (DMSO-*d*₆): δ 3.08 (s, 6H), 7.64–7.68 (m, 2H), 8.42–8.45 (m, 2H), 8.66 (s, 2H). MS (EI⁺): *m/z* 294 (M⁺). Mp: >300 °C.

Synthesis of 9,10-Dimethyl-2,3-anthracenedicarboxylic Anhydride (8). A suspension of **7** (645 mg, 2.19 mmol) in acetic anhydride (110 mL) was refluxed for 10 min. The clear solution was cooled to 4 °C to afford **8** as a red precipitate (367 mg, yield 61%). ¹H NMR (CDCl₃): δ 3.23 (s, 6H), 7.72–7.75 (m, 2H), 8.42–8.46 (m, 2H), 9.12 (s, 2H). MS (EI⁺): *m/z* 276 (M⁺). Mp: 278 °C dec.

Synthesis of 5,10-Dimethyl-3',6'-bis(acetyloxy)spiro[anthra[2,3-*c*]furan-1(3H),9'-[9H]-xanthen]-3-one (DMAX-diAc), 3',6'-Bis(acetyloxy)spiro[naphtho[2,3-*c*]furan-1(3H),9'-[9H]-xanthen]-3-one (NX-diAc), and 3',6'-Bis(acetyloxy)spiro[anthra[2,3-*c*]furan-1(3H),9'-[9H]-xanthen]-3-one (AX-diAc). Compound **8** (367 mg, 1.33 mmol) was added to a solution of resorcinol (681 mg, 6.18 mmol) in methanesulfonic acid (6.6 mL). The resulting suspension was heated under Ar at 85 °C for 24 h. The cooled mixture was poured into 7 volumes of ice water, followed by filtration. The filtrate was dried at 60 °C in vacuo, and the residue was diacetylated. The product, acetic anhydride (8 mL), and pyridine (4 mL) were stirred for 10 min at room temperature under an Ar atmosphere. The resulting mixture was poured

(16) (a) Fairbourne, A. *J. Chem. Soc.* **1921**, 119, 1573–1582. (b) Elbs, K.; Eurich, H. *Ber. Dtsch. Chem. Ges.* **1887**, 20, 1361–1363.

(17) Rimmer, R. W.; Christiansen, R. G.; Brown, R. K.; Sandin, R. B. *J. Am. Chem. Soc.* **1950**, 72, 2298–2299.

into 2% HCl at 0 °C and extracted with CH₂Cl₂. The organic layer was washed with brine, dried over Na₂SO₄, filtered, and evaporated. The residue was recrystallized from benzene to afford DMAX-diAc (294 mg, yield 48%). ¹H NMR (CDCl₃): δ 2.31 (s, 6H, acetyl), 2.99 (s, 3H, CH₃), 3.29 (s, 3H, CH₃), 6.79 (dd, 2H, *J* = 8.7, 2.2 Hz, H₂, H₇), 6.92 (d, 2H, *J* = 8.7 Hz, H₁, H₈), 7.14 (d, 2H, *J* = 2.2 Hz, H₄, H₅), 7.59–7.62 (m, 2H, H₇, H₈), 8.11 (s, 1H, H₁₁), 8.30–8.42 (m, 2H, H₆, H₉), 9.20 (s, 1H, H₄). ¹³C NMR (CDCl₃): δ 14.80 (CH₃), 14.85 (CH₃), 21.1 (CH₃(Ac)), 82.3 (C₁), 110.3 (C₄, C₅), 117.8 (C₂, C₇), 117.9 (C_{8a}, C_{9a}), 121.2 (C₁₁), 123.1 (C_{3a}), 125.45 (C₄), 125.48 (C₆/C₉), 125.7 (C₆/C₉), 126.0 (C₇/C₈), 126.8 (C₇/C₈), 129.6 (C₁, C₈), 130.0 (C₅/C₁₀), 130.6, 131.9, 132.0, 132.5 (C_{4a}, C_{5a}, C_{9a}, C_{10a}), 144.4 (C_{11a}), 151.6 (C_{4a}, C_{10a}/C₃, C₆), 152.0 (C_{4a}, C_{10a}/C₃, C₆), 168.9 (CO(Ac)), 169.1 (C₃). MS (FAB⁺): *m/z* 461 (M⁺ + 1). Mp: 280 °C dec. Anal. Calcd for C₃₅H₂₈O₇: C, 74.99; H, 4.44; N, 0.00. Found: C, 74.82; H, 4.72; N, 0.00.

NX-diAc and AX-diAc were similarly prepared from 2,3-naphthalenedicarboxylic anhydride and 2,3-anthracenedicarboxylic anhydride in 32% and 25% yield, respectively.

NX-diAc. ¹H NMR (CDCl₃): δ 2.31 (s, 6H, acetyl), 6.78 (dd, 2H, *J* = 8.6, 2.2 Hz, H₂, H₇), 6.86 (d, 2H, *J* = 8.6 Hz, H₁, H₈), 7.12 (d, 2H, *J* = 2.2 Hz, H₄, H₅), 7.62–7.66 (m, 3H, H₆, H₇, H₉), 7.82–7.85 (m, 1H, H₅/H₈), 8.12–8.14 (m, 1H, H₅/H₈), 8.61 (s, 1H, H₄). ¹³C NMR (CDCl₃): δ 21.1 (CH₃(Ac)), 81.9 (C₁), 110.3 (C₄, C₅), 117.4 (C_{8a}, C_{9a}), 117.7 (C₂, C₇), 123.6 (C₉), 124.0 (C_{3a}), 126.7 (C₄), 127.6 (C₆/C₇), 128.7 (C₅/C₈), 129.3 (C₁, C₈), 129.4 (C₆/C₇), 130.0 (C₅/C₈), 133.5 (C_{4a}/C_{8a}), 136.8 (C_{4a}/C_{8a}), 147.3 (C_{9a}), 151.5 (C_{4a}, C_{10a}/C₃, C₆), 152.0 (C_{4a}, C_{10a}/C₃, C₆), 168.0 (C₃, CO(Ac)). MS (FAB⁺): *m/z* 467 (M⁺ + 1). Mp: 241 °C dec. Anal. Calcd for C₂₈H₁₈O₇: C, 72.10; H, 3.89; N, 0.00. Found: C, 71.80; H, 3.89; N, 0.00.

AX-diAc. ¹H NMR (CDCl₃): δ 2.31 (s, 6H, acetyl), 6.80 (dd, 2H, *J* = 8.7, 2.2 Hz, H₂, H₇), 6.94 (d, 2H, *J* = 8.7 Hz, H₁, H₈), 7.14 (d, 2H, *J* = 2.2 Hz, H₄, H₅), 7.55–7.58 (m, 2H, H₇, H₈), 7.80 (s, 1H, H₁₁), 7.98–8.08 (m, 2H, H₆, H₉), 8.34 (s, 1H, H₄/H₅/H₁₀), 8.42 (s, 1H, H₄/H₅/H₁₀), 8.76 (s, 1H, H₄/H₅/H₁₀). ¹³C NMR (CDCl₃): δ 21.1 (CH₃(Ac)), 82.0 (C₁), 110.3 (C₄, C₅), 117.76 (C₂, C₇), 117.83 (C_{8a}, C_{9a}), 123.8 (C_{3a}), 123.9 (C₁₁), 126.7 (C₇/C₈), 127.4 (C₇/C₈), 127.5 (C₄/C₅/C₁₀), 128.1 (C₄/C₅/C₁₀), 128.2 (C₆/C₉), 128.5 (C₆/C₉), 129.4 (C₁, C₈), 129.6 (C₄/C₅/C₁₀), 130.9, 132.4, 133.3, 133.6 (C_{4a}, C_{5a}, C_{9a}, C_{10a}), 145.4 (C_{11a}), 151.5 (C_{4a}, C_{10a}/C₃, C₆), 152.0 (C_{4a}, C_{10a}/C₃, C₆), 168.7 (C₃), 168.9 (CO(Ac)). MS (FAB⁺): *m/z* 517 (M⁺ + 1).

Synthesis of DMAX-9,10-endoperoxide-diAc (DMAX-EP-diAc). A solution of DMAX (104 mg, 0.23 mmol) in DMSO (20 mL) was added to an aqueous solution (180 mL) of NaOH (12.5 mM), NaHCO₃ (6.5 mM), Na₂CO₃ (12.5 mM), and Na₂MoO₄·2H₂O (55.2 mM). Throughout the reaction, the temperature was maintained at about 20 °C. Next, 30% H₂O₂ (5 mL) was added to the solution, and the mixture was stirred for 15 min. Another 5 mL of H₂O₂ was allowed to react in the same way, and the reaction was monitored by HPLC to check the complete conversion of DMAX to DMAX-EP. The mixture was cooled to 0 °C and was acidified to pH ~2.5 with cold 2 M phosphoric acid. The resulting mixture was extracted with ether. The organic layer was washed with brine, dried over MgSO₄, filtered, and evaporated. The residue was then diacetylated by the same method as in the case of DMAX-diAc. After evaporation, the crude compound was purified by silica gel chromatography, eluted with CH₂Cl₂, to give DMAX-EP-diAc (59 mg, yield 45%). ¹H NMR (CDCl₃): δ 2.06 (s, 3H, CH₃), 2.26 (s, 3H, CH₃), 2.28 (s, 3H, acetyl), 2.33 (s, 3H, acetyl), 6.67–6.74 (m, 2H, H₁, H₂/H₇, H₈), 6.84–6.99 (m, 2H, H₁, H₂/H₇, H₈), 7.06–7.13 (m, 2H, H₄, H₅), 7.14 (s, 1H, H₁₁), 7.30–7.49 (m, 4H, H₆, H₇, H₈, H₉), 8.01 (s, 1H, H₄). ¹³C NMR (CDCl₃): δ 13.9 (CH₃), 14.0 (CH₃), 21.10 (CH₃(Ac)), 21.15 (CH₃(Ac)), 79.5 (C₅/C₁₀), 79.7 (C₅/C₁₀), 81.8 (C₁), 110.4 (C₄/C₅), 110.5 (C₄/C₅), 115.8 (C_{8a}/C_{9a}), 115.8 (C_{8a}/C_{9a}), 116.6 (C₁₁), 117.3 (C₄), 117.8 (C₂/C₇), 118.0 (C₂/C₇), 121.2 (C₆/C₉), 121.6 (C₆/C₉), 125.1 (C_{3a}), 128.1 (C₇/C₈), 128.2 (C₇/C₈), 129.1 (C₁/C₈), 129.4 (C₁/C₈), 139.1, 139.7, 143.5, 148.9, 152.6 (C_{4a}, C_{5a}, C_{9a}, C_{10a}, C_{11a}), 151.4, 151.5, 152.1, 152.3 (C_{4a}/C_{10a}/C₃/C₆), 168.8 (C₃), 168.9 (CO(Ac)), 170.0 (CO(Ac)). MS (FAB⁺): *m/z* 577 (M⁺ + 1). Mp: 196 °C dec.

Synthesis of 9-[2-(3-Carboxy-9,10-dimethyl)anthryl]-6-hydroxy-3H-xanthen-3-one (DMAX), DMAX-9,10-endoperoxide (DMAX-

EP), 9-[2-(3-Carboxy)naphthyl]-6-hydroxy-3H-xanthen-3-one (NX), and 9-[2-(3-Carboxy)anthryl]-6-hydroxy-3H-xanthen-3-one (AX). DMAX-diAc (30 mg, 65.1 μmol) was dissolved in THF (5 mL) and MeOH (5 mL), and this solution was stirred with 15% aqueous ammonia (1.4 mL) for 5 min in the dark. The reaction mixture was poured into 60 mL of cold water, and the whole was acidified to pH 2 with 10% HCl and then evaporated to a small volume to remove THF/MeOH. The resulting mixture was extracted with ether. The organic layer was washed with brine, dried over MgSO₄, filtered, and evaporated to yield DMAX (18 mg, yield 60%). ¹H NMR (DMSO-*d*₆): δ 3.15 (s, 3H), 3.17 (s, 3H), 6.49–6.52 (m, 2H), 6.65–6.69 (m, 4H), 7.63–7.67 (m, 2H), 8.14 (s, 1H), 8.35–8.50 (m, 2H), 9.09 (s, 1H). MS (FAB⁺): *m/z* 461 (M⁺ + 1). Mp: 236 °C dec.

DMAX-EP, NX, and AX were similarly prepared from DMAX-EP-diAc, NX-diAc, and AX-diAc in 100, 100, and 83% yield, respectively.

DMAX-EP. ¹H NMR (DMSO-*d*₆): δ 3.15 (s, 3H), 3.16 (s, 3H), 6.42 (d, 2H, *J* = 1.1 Hz), 6.60–6.68 (m, 4H), 7.32 (s, 3H), 7.37–7.56 (m, 4H), 8.02 (s, 1H). MS (FAB⁺): *m/z* 493 (M⁺ + 1). Mp: 172 °C dec.

NX. ¹H NMR (DMSO-*d*₆): δ 6.51 (dd, 2H, *J* = 2.3, 8.6 Hz), 6.60 (d, 2H, *J* = 8.6 Hz), 6.68 (d, 2H, *J* = 2.2 Hz), 7.67–7.70 (m, 2H), 7.83 (s, 1H), 8.00–8.31 (m, 2H), 8.71 (s, 1H). MS (FAB⁺): *m/z* 383 (M⁺ + 1). Mp: 195 °C dec.

AX. ¹H NMR (DMSO-*d*₆): δ 6.52 (dd, 2H, *J* = 2.4, 8.6 Hz), 6.66–6.70 (m, 4H), 7.59–7.62 (m, 2H), 7.97 (s, 1H), 8.04–8.20 (m, 2H), 8.67 (s, 1H), 8.93 (s, 1H), 9.03 (s, 1H). MS (FAB⁺): *m/z* 433 (M⁺ + 1). Mp: 195 °C dec.

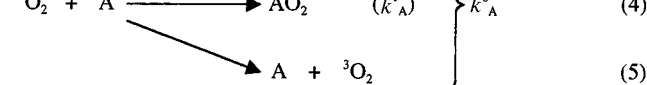
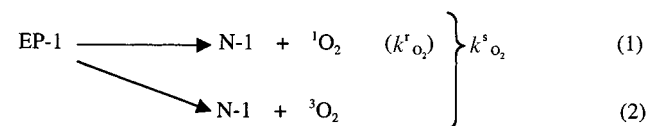
Computational Methods. Semiempirical PM3 calculations were carried out using Spartan (version 5.0) on SGIO2. Several starting geometries were used for the geometry optimization to ensure that the optimized structure corresponds to a global minimum.

Fluorometric Analysis. The slit width was 2.5 nm for both excitation and emission. The photon multiplier voltage was 950 V. Relative quantum efficiencies of fluorescence of fluorescein derivatives were obtained by comparing the area under the corrected spectrum of the test sample excited at 492 nm in 0.1 M NaOH with that of a solution of fluorescein, which has a quantum efficiency of 0.85 according to the literature.¹⁸

In the experiment to measure the reaction rate constant, the slit width was 7.5 nm for excitation and 3.5 nm for emission, and the photon multiplier voltage was 750 V. DMAX and DPAX-1 were dissolved in DMSO to obtain a 10 mM stock solution. A 3 μL aliquot of the stock solution was added to 3 mL of sodium phosphate buffer (100 mM, pH 7.4) with stirring. After 5 min, 30 μL of DMSO solution in which EP-1 was dissolved was added.

HPLC Analysis. HPLC analyses were performed on an Inertsil ODS-3 (4.6 × 250 mm) column using an HPLC system composed of a Jasco 880-PU pump and a Jasco 870-UV detector.

Determination of Reaction Rate Constant. The reaction scheme for reaction of an acceptor (A), DMAX or DPAX-1, with ¹O₂ in solution is expressed as follows:



r is the probability of the reaction of A with ¹O₂ (= *k*^{*t*}_A/*k*^{*s*}_A), and *γ* is the probability of formation of ¹O₂ from EP-1 (= *k*^{*t*}_{O₂}/*k*^{*s*}_{O₂}). The values of *k*_d (5.00 × 10⁵ s⁻¹), *k*^{*s*}_{O₂} (4.9 × 10⁻⁴ s⁻¹), and *γ* (0.82) are from the

literature.^{10,14b} DMA and DPA are reported to be efficient acceptors, so they can react without deactivation reaction of $^1\text{O}_2$ (eq 5); thus, r is close to 1. The data of time-dependent fluorescence increases of DMAX and DPAX-1 upon reaction with various concentrations of EP-1 were fitted to eq 6,

$$F = F_{\max} (1 - e^{-kt}) \quad (6)$$

where F is the fluorescence intensity and F_{\max} is the maximum fluorescence intensity. The initial reaction rate (R) is given by

$$R = kF_{\max}/\epsilon\phi \quad (7)$$

where the value of $\epsilon\phi$ is estimated from the relationship between the fluorescence intensity of DMAX-EP or DPAX-1-EP and the concentration. Using the initial reaction rate, the following equation can be written:

$$R = k_{\text{O}_2}^s[\text{EP-1}]\gamma \frac{k_{\text{A}}^r[\text{A}]}{k_{\text{A}}^r[\text{A}] + k_{\text{d}}} \quad (8)$$

Thus, the rate constant for reaction of A with $^1\text{O}_2$ is given by

$$k_{\text{A}}^r = \frac{R k_{\text{d}}}{[\text{A}](k_{\text{O}_2}^s[\text{EP-1}]\gamma - R)} \quad (9)$$

Acknowledgment. This work was supported by research grants from the Ministry of Education, Science, Sports and Culture of Japan (Grant Nos. 11794026, 12470475, and 12557217 to T.N., 10771238 and 12771349 to Y.U.). We thank Professor W. Nakanishi (Wakayama University) for helpful discussion.

JA0035708